Journal of Biomedical Optics

BiomedicalOptics.SPIEDigitalLibrary.org

Photocontrolled nitric oxide release from two nitrosylruthenium isomer complexes and their potential biomedical applications

Jiao Liu
Qingqing Duan
Jianru Wang
Zhen Song
Xiaoyan Qiao
Hongfei Wang

SPIE.

Photocontrolled nitric oxide release from two nitrosylruthenium isomer complexes and their potential biomedical applications

Jiao Liu,[a,†] Qingqing Duan,[b,†] Jianru Wang,[b,c] Zhen Song,[a] Xiaoyan Qiao,[d] and Hongfei Wang[a,b,*]
[a]Shanxi University, Institute of Molecular Science, Key Laboratory of Chemical Biology and Molecular Engineering of the Education Ministry, 92 Wucheng Road, Taiyuan 030006, China
[b]Shanxi University, Institute of Opto-Electronics, State Key Lab of Quantum Optics and Quantum Optics Devices, 92 Wucheng Road, Taiyuan 030006, China
[c]Shanxi Medical University, Institute of Basic Medicine, 56 Xinjiannan Road, Taiyuan 030012, China
[d]Shanxi University, College of Physics & Electronics Engineering, 92 Wucheng Road, Taiyuan 030006, China

Abstract. Nitric oxide (NO) has key regulatory roles in various biological and medical processes. The control of its local concentration, which is crucial for obtaining the desired effect, can be achieved with exogenous NO donors. Release of NO from metal-nitrosyl complexes upon exposure to light is a strategy that could allow for the site-specific delivery of the reactive species NO to physiological targets. The photodissociation of NO from two nitrosylruthenium(II) isomer complexes {cis- and trans-$[Ru(OAc)(2mqn)_2NO]$} was demonstrated by matrix-assisted laser desorption ionization time-of-flight mass spectrometry spectra, and electron paramagnetic resonance spectra further prove the photoinduced NO release by spin trapping of NO free radicals upon photoirradiation. Real-time NO release was quantitatively measured by electrochemistry with an NO-specific electrode. The quantitative control of NO release from $[Ru(OAc)(2mqn)_2NO]$ in aqueous solutions was done by photoirradiation at different wavelengths. Both isomers show photoinduced damage on plasmid DNA, but the trans isomer has higher cytotoxicity and photocytotoxicity activity against the HeLa tumor cell line than that of the cis isomer. Nitrosylruthenium(II) complex, with 8-quinolinol derivatives as ligands, has a great potential as a photoactivated NO donor reagent for biomedical applications. [DOI: 10.1117/1.JBO.20.1.015004]

Keywords: nitrosyl; ruthenium complex; nitric oxide donor; photoirradiation; DNA; cell.

Paper 140639RR received Oct. 2, 2014; accepted for publication Dec. 17, 2014; published online Jan. 26, 2015.

1 Introduction

Nitric oxide (NO) has been shown to be an important signaling molecule in a wide variety of physiological and pathological processes, such as the modulation of the immune and endocrine response, cardiovascular control, regulation of blood pressure, neurotransmission, induction of apoptosis, and inhibition of tumor growth.[1–5] Since these discoveries, research efforts have been directed toward development of exogenous NO donors that can deliver NO to specific biological targets. Various NO donors have been developed and have been clinically used as drugs, including organic nitrites and nitrates, nitrosothiols, diazeniumdiolates (NONOates), and transition metal based NO donors, such as sodium nitroprusside.[6–10] However, these compounds and complexes release NO spontaneously; controlled or favorably triggered release of NO at a selected site is the key way for successful employment of an NO donor in regulation of physiological processes and treatment of diseases.

Metal nitrosyl complexes release NO only when exposed to light, which makes them candidates of choice with the advent of photodynamic therapy (PDT). Compared to most alternative metal complexes, ruthenium nitrosyls are especially appealing and provided the most promising candidates in relation to their inherent stability in aqueous media and modest photosensitivity.[11–13] The photochemical activation of these complexes is utilized for clinical therapy for targeted cancer and other diseases.[14–16] Furthermore, the reactivities and biological properties of metal complexes significantly vary depending on their isomeric structures. A classic example of metal-based anticancer drugs with dramatically different biological activities is cis- and trans-platin, of which cis-platin is the widely clinically used anticancer agent, while its corresponding trans isomer shows less anticancer activities. Recently, several classes of trans-configured complexes have been reported to exhibit higher cytotoxicities, which lack cross-resistance to cis-platin. An example of such complexes is $(H_2trz)[trans\text{-}RuCl_4(Htrz)_2]$, where Htrz = 1 H-1,2,4-triazole.[17–19] Two other excellent trial drugs, $(H_2im)[trans\text{-}RuIII\,Cl_4(DMSO)(Him)]$ (NAMI-A) and $(H_2ind)[trans\text{-}RuIIICl_4(Hind)_2]$ (KP1019), are also currently undergoing human clinical trials.[20–23]

In this study, the photoinduced NO release by two geometrical isomers of nitrosylruthenium(II) complex with 2mqn (H2mqn = 2-methyl-8-quinolinol) as a ligand was investigated. Figure 1 presents the structures of the cis and trans isomers as well as that of the H2mqn ligand. The photodissociation of $[Ru(OAc)(2mqn)_2NO]$ isomers and quantitative determination of NO were characterized by matrix-assisted laser desorption/ionization time-of-flight mass spectrometry (MALDI-TOF MS). The spin trapping of NO-free radicals was conducted

*Address all correspondence to: Hongfei Wang, E-mail: wanghf@sxu.edu.cn

†First and second authors contributed to this work equally.

0091-3286/2015/$25.00 © 2015 SPIE

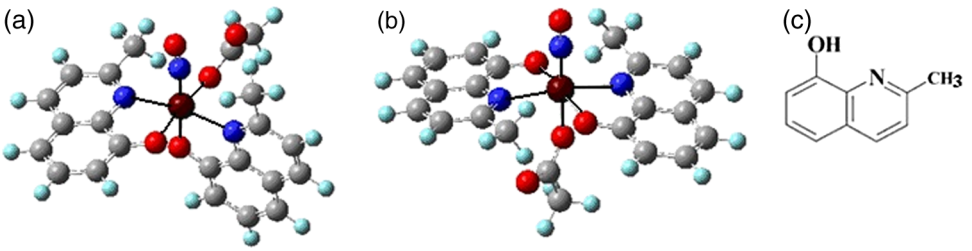

Fig. 1 Schematic structures of the (a) cis and (b) trans isomers. (c) Structure of ligand H2mqn.

via electron paramagnetic resonance (EPR) spectroscopy, and the NO release was monitored by electrochemistry using an NO-specific electrode. The basic method was developed to quantitatively control NO release in aqueous solutions by photoirradiation. Furthermore, density functional theory (DFT) calculations were also performed to understand the photodissociation of NO, the photoinduced damage on plasmid DNA, and the photoincreased cytotoxicity against tumor cell lines by these isomer complexes. This study provided insight into the photocontrolled NO release and its potential applications in photobiology and medicine.

2 Methods and Materials

2.1 *Chemicals and Reagents*

Chemical reagents and solvents were purchased from local available sources. The calf thymus DNA and supercoiled (CsCl purified) pBR322DNA were purchased from Takara (Japan). The spin trapper N-methyl-D-glucamine dithiocarbamate (MGD) and 5,5-dimethyl-1-pyrroline N-oxide (DMPO) were purchased from Dojindo (Japan). 2,2,6,6-Tetramethylpiperidine 1-oxyl (TEMPO) was purchased from Sigma.

Cis-$[Ru(OAc)(2mqn)_2NO]$ and trans-$[Ru(OAc)(2mqn)_2NO]$ complexes were synthesized following a previously described procedure.[24,25] Hydrous nitrosylruthenium trichloride (0.5 mmol) and 2-methyl-8-quinolinol (2.0 mmol) were mixed in 0.1 M acetic acid aqueous solution and the solution was refluxed for 5 h under dinitrogen in the dark. After cooling, the precipitate was collected by filtration and dried under vacuum. The crude product was chromatographically separated using a silica-gel column. The cis isomer complex was eluted from the major band with 30 vol.% ethylacetate – CH_2Cl_2. The cis complex (0.1 mmol) was dissolved in CH_2Cl_2, and the solution was irradiated with an Xe lamp through a combination of a UV cut filter and a water filter for 5 h at room temperature. After the solvent was removed, the trans isomer was chromatographically separated using ethylacetate – CH_2Cl_2 as an eluent with a yield of 20%. The cis and trans isomer complexes were confirmed through ^1H NMR spectra using a Bruker 600 M spectrometer.

2.2 *Instruments and Measurements*

MALDI-TOF MS measurements were performed using a BIFLEX III MALDI-TOF mass spectrometer (Bruker Daltonics) equipped with a nitrogen laser ($\lambda = 337$ nm). The mass spectra (20 summed shots) were acquired in the reflector mode with a 19 kV accelerating voltage and a 20 kV reflector voltage. CH_3CN matrix was used for the MALDI experiment. The matrix solution and analyte solution were mixed and the result was spotted on the MALDI target plate. After air-drying, the samples were analyzed.

EPR spectra were obtained at room temperature by using a Bruker ESP-300E spectrometer at 9.8 GHz, X-band, with a 100 Hz field modulation. Cis or trans isomers in DMSO at 5 mM, mixed with 2 mM$Fe(MGD)_2$, was quantitatively injected into quartz capillaries and then was illuminated in the cavity of the EPR spectrometer with an Nd:YAG laser at 532 nm (5 to 6 ns of pulse width, 10 Hz of repetition, 30 mJ/pulse). Nanosecond laser pulses for excitation at 355 nm were generated by an Nd^{3+}: YAG laser. The excitation energy of each pulse was ~3 mJ. All measurements were performed at room temperature.

Real-time measurements of NO were conducted by electrochemistry on TBR4100 four-channel free radical analyzer (World Precision Instruments, USA) equipped with a wide range NO-selective electrode (WPI). The ISO-NOP NO meter (2 mm) was vertically and directly immersed inside the quartz cuvette containing 10 μM complex solution in 10 mM phosphate buffer at pH 7.4. The TBR4100 analyzer is interfaced with PC via Lab-Trax system. The data are acquired in real time by using the LabScribe software. To avoid any reaction before the light irradiation, the samples were protected from light by using an aluminum foil. The NO release profile was constructed by plotting the current versus time. The current of the buffer solution was set as a zero baseline to calculate the current increment. The complex solution of different isomers in the quartz cuvette was irradiated by an Xe lamp (300 W, Beijing NBeT Corp.) at the central wavelengths of 254, 420, and 550 nm with a bandwidth of 40 nm by several band-pass filters. The irradiation power measured by an optical power meter (LPE-1B, Physcience Opto-Electronics, Beijing) was kept constant at 0.2 W/cm^2 by adjusting the lamp current and the distance between the light source and sample.

2.3 *DFT Calculations*

DFT calculations were performed using the Gaussian 09 program package.[26] The original coordinates of the cis and trans isomer atoms were obtained from the crystal structures determined via x-ray diffraction. Visualization was performed using Gaussian view 5.[27] All geometries were fully optimized without imposing any symmetry constraint with the Becke's three-parameter hybrid function with the Lee-Yang-Parr correlation function.[28,29] The standard Wadt-Hay realistic effective core potentials were incorporated in the Gaussian 09 to describe the core electrons of the Ru atom. The 6-311G (d, p) was used for the ligand atoms. The frequency calculated at the DFT level was compared with the experimental frequency to check whether the stationary points from the geometry optimization were in real minima.

2.4 *Photoinduced DNA Damage*

The photoinduced DNA damage by the two isomers was investigated via agarose gel electrophoresis. A supercoiled pBR322 DNA (0.2 μg) was mixed with a two isomer complexes solution at 50 mM, respectively, and incubated at 37°C for 30 min in the dark. The solution was then irradiated at room temperature by an Xe light source with 420-nm bandpass filters (~200 mW/cm^2) for 0.5 h. The samples were analyzed via electrophoresis for 1 h at 90 V on a 1% agarose gel in buffer (40 mM Tris—CH_3COOH, 1 mM ethylenediaminetetraacetic acid, pH = 8.0). The gel was stained with 1 μgmL^{-1} EB and photographed under UV light. The mechanistic investigations of pBR322DNA were conducted using free radical scavengers, sodium azide (NaN_3, 3 mM), which were added to pBR322 DNA prior to the addition of the complex.

2.5 *Cytotoxic Activity*

A HeLa tumor cell line was used in this study with standard 3-(4,5-dimethylthiazol-2-yl)-2,5-diphenyltetrazolium bromide (MTT) assay procedures. Cells were seeded in 96-well plates (1×10^3/well) in growth medium (100 μL) and incubated at 37°C under a 5% CO_2 atmosphere for 24 h, and then were treated with various concentrations of complexes in a mixture of growth medium. The complexes were dissolved in DMSO and diluted with Roswell Park Memorial Institute medium 1640, and then added to the wells at a different final concentration. The concentration of DMSO was controlled <1%. Control wells were prepared by the addition of a culture medium (100 μL) without complexes, which was also incubated at 37°C under a 5% CO_2 atmosphere for 24 h. MTT (20 μl of 5 mg/ml) was added to each well, and then the plates were further incubited for 4 h. The culture medium was finally discarded, and 150 μL of DMSO was added to solubilize the MTT. The solution absorbance at 490 nm was measured with a microplate-reader. The IC_{50} values of complexes were determined by plotting the viability percentage versus concentration on a logarithmic scale and reading off the concentration at which 50% of cells were viable relative to the control.

For comparing the effect of photoirradiation on the cytotoxic activity of isomer complexes, cell cultures upon photoirradiation were performed at the same conditions. After adding 20 μL complex isomers in a mixture of growth medium at various concentrations, the cells were incubated at 37°C under a 5% CO_2 atmosphere for 4 h; then the plates were irradiated with a light source of 420 nm (~0.2 W/cm^2) for 30 min and again were incubated at 37°C in a 5% CO_2 incubator for 24 h. Upon completion of the incubation, a stock MTT dye solution (20 μL, 5 mg/mL) was added to each well. After 4 h of incubation, the culture medium was finally discarded, and 150 μL of DMSO was added to solubilize the MTT. The optical density of each well was then measured using a microplate spectrophotometer at 490 nm. Each experiment was repeated at least three times to obtain the mean values.

3 Results

3.1 *Photoinduced NO Release*

3.1.1 *MALDI-TOF MS spectra*

To identify the products of photoinduced fragmentation, MALDI-TOF MS was used to analyze the isomer complexes. Two main mass signals appearing in MALDI-TOF MS spectrum are attributed to the fragments of $[Ru(II)(2mqn)_2NO]^+$ (m/z447.9 ± 0.1, $m_{theor} = 448.0$) and $[Ru(III)(2mqn)_2]^+$ (m/z417.9 ± 0.1, $m_{theor} = 418.0$). The calculated mass of $[Ru(OAc)(2mqn)_2NO]$ was 507.0 Da, and the fragment of $[Ru(II)(2mqn)_2NO]^+$ was formed by the loss of the –OAc group with a mass of 59.0 Da. The other fragment of $[Ru(III)(2mqn)_2]^+$ was formed by the loss of –OAc and –NO with a mass of 30.0 Da. The molecular ion peak of $[Ru(OAc)(2mqn)_2NO]$ was not observed for both isomers upon photoexcitation, indicating that $[Ru(OAc)(2mqn)_2NO]$ was completely dissociated by losing the –OAc group and $[Ru(II)(2mqn)_2NO]^+$ further dissociated to $[Ru(III)(2mqn)_2]^+$ by losing the NO group upon photoirradiation.

3.1.2 *EPR spectroscopy*

Iron(II)-N-methyl-D-glucamine dithiocarbamate $[Fe(MGD)_2]$ is commonly used to trap NO because of its high probability of adduct formation and the high stability of its spin adduct. Spin trapping, together with EPR spectroscopy by using $Fe(MGD)_2$ is considered as one of the best methods for detecting $NO^{\bullet}$ in real time and at its generation site.[30,31] Both $[Ru(OAc)(2mqn)_2NO]$ isomers produced NO free radicals through photoexcitation at either 355 or 532 nm.

Figure 2 shows the characteristic triplet signal with a hyperfine splitting constant (hfsc) value of $a_N = 12.78$ G and a g-factor of $g = 2.041$, which is consistent with the literature report for NO-Fe^{2+}-MGD adduct.[32,33] More free radical molecules were generated at the photoexcitation of 355 nm than at the photoexcitation of 532 nm, and the trans isomers produced a little more free radicals at a photoexcitation of 355 nm than the cis isomers at the same conditions.

3.1.3 *DFT calculations*

DFT calculations were successfully used for investigating the reactivities of ruthenium complexes.[34] Figure 3 shows the energy levels and contour plots of the frontier orbitals of cis- and trans-$[Ru(OAc)(2cqn)_2NO]$ complexes. For both isomers, the highest occupied molecular orbital (HOMO) was a 2mqn ligand-based π orbital with minimal Ru (d) and NO (p), whereas the lowest unoccupied molecular orbital (LUMO) was the antibonding overlap of Ru (d) and $\pi * \mathrm{NO}(p)$. The orbital analyses indicate that the direct excitation of an electron from a bonding $\pi_{2mqn} - d\pi$ orbital to an antibonding $\pi*_{NO} - d\pi$ orbital causes the photorelease of NO from ruthenium–nitrosyls.

The previous studies on ruthenium polypyridyl complexes {such as $[[Ru(bpy)_{3-n}(L)_n]^{2+}]$, L = diimine ligands} found that the HOMO was centered on the ruthenium represented by Ru (d) t_{2g}, whereas the LUMO was localized on the bpy ($\pi*$). Metal-to-ligand charge transfer transition has an important function in photochemical and photophysical processes of these ruthenium-N-donor complexes.[35,36] The different transition contributions of the HOMOs—LUMOs of Ru complexes lead to different pathways and patterns for the exited state, thereby resulting in the formation of different free radical species.

As shown in Fig. 3, the calculated energy of the HOMO–LUMO gap for the trans isomer was smaller than that of the cis isomer, which suggests that the trans isomer is more active upon photoirradiation, agreeing with the experimental observations.

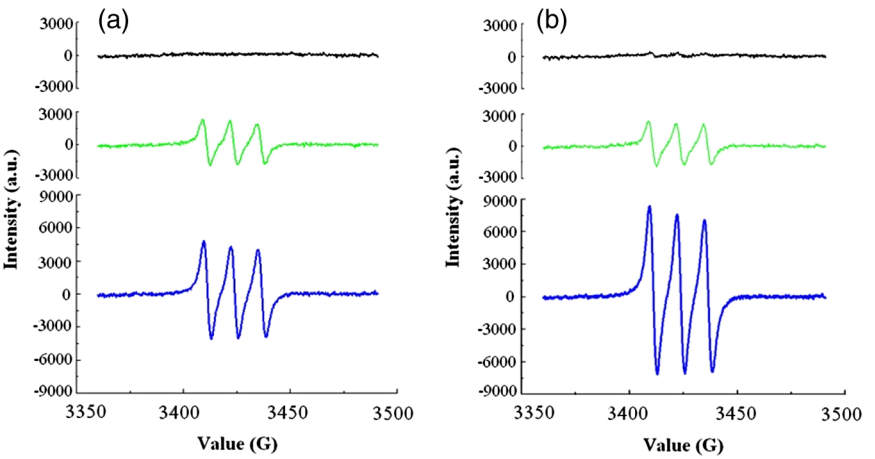

Fig. 2 Triplet electron paramagnetic resonance signals caused from nitric oxide (NO) trapping by Fe^{2+}-N-methyl-D-glucamine dithiocarbamate for the (a) cis and (b) trans isomer complexes upon irradiation with 355- (blue line) and 532-nm (green line) lasers. Dark control (black line) means no light irradiation at identical conditions.

3.2 *Real-Time Measurement of NO Release*

Real-time NO release was measured by the electrochemistry with the free radical analyzer. The NO release increased for both $[Ru(OAc)(2mqn)_2NO]$ isomers at the photoexcitation of 550, 420, and 254 nm, and white light. Photoirradiation wavelength positions are selected according to the measured absorption spectra: around the absorption peak in the visible region (420 nm); around the lower-absorption region (550 nm); around the absorption peak in the UV region (254 nm); and, finally, white light containing all wavelengths in the visible region. As shown in Fig. 4, the amount of released NO increased as the irradiated wavelength moving from visible region to UV region reached a maximum under white light irradiation; the amount of NO production increased as the absorbance increased in absorption spectra. Therefore, the NO release could be controlled by varying the irradiation wavelength. Moreover, the trans isomers produced slightly more NO free radicals than the cis isomers at the same conditions.

3.3 *Photoinduced DNA Damage*

Since DNA was identified as the primary target of metal-based anticancer agents, considerable attention has been drawn into the interaction of ruthenium complexes with DNA for the potential of ruthenium complexes as chemotherapeutic agents. Further studies on the mechanism show that ruthenium complexes containing polypyridyl, imidazole, and β-carboline derivatives are antiproliferative and able to induce caspase-dependent apoptosis in cancer cells with mitochondrial dysfunction.[37–40] The photoinduced effect and damage of the $[Ru(OAc)(2mqn)_2NO]$ isomers on plasmid DNA were monitored via agarose gel electrophoresis. When circular plasmid DNA is subjected to electrophoresis, a relatively fast migration is generally observed for the intact supercoiled Form I. While the scission occurs on one strand (nicking), the supercoil relaxes to generate a slower-moving, open-circular Form II. If DNA conformation was further changed, a broader linear Form III between Forms I and II is generated.[41–43]

Figure 5 shows the photoinduced damage of pBR322 DNA by $[Ru(OAc)(2mqn)_2NO]$ isomers. No change was observed in the control experiment (Lane 1) compared with the incubation of the plasmid DNA with the complex in the dark (Lane 2). After irradiation at 420 nm for 30 min, 50 μM of the complex caused an apparent conformational change of DNA because Form I disappeared and Form III (Lane 3) appeared. These results demonstrate that DNA damage occurred through the photoinduced reaction pathway. In the presence of NaN_3, a well-known scavenger of singlet oxygen ($^1O_2$), there is no evident inhibition of

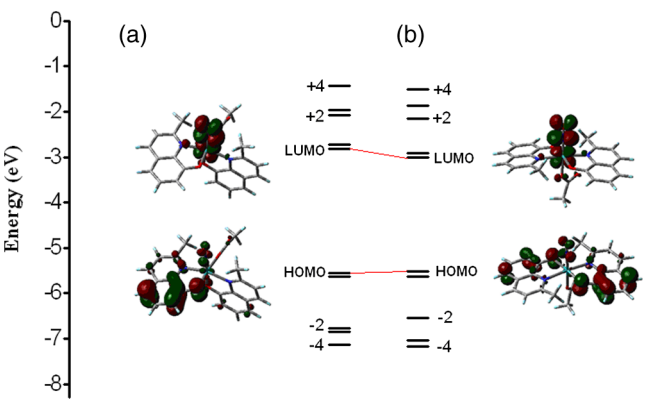

Fig. 3 Contour diagrams of calculated LUMO (top) and HOMO (bottom) of (a) cis-$[Ru(OAc)(2mqn)_2NO]$ and (b) trans-$[Ru(OAc)(2mqn)_2NO]$. Positive values of wave function are shown in green.

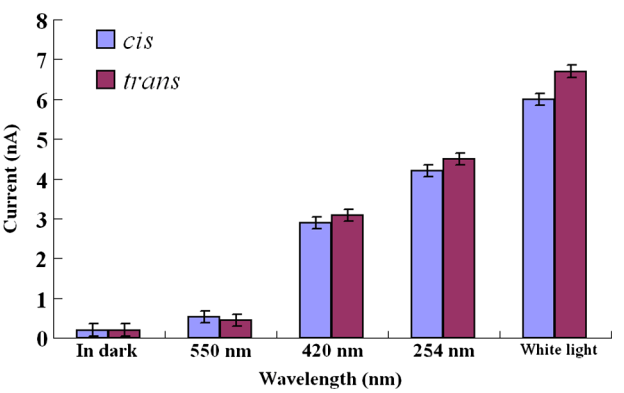

Fig. 4 Real-time measurement of NO release measured with NO-specific electrode upon photoirradiation at different wavelengths.

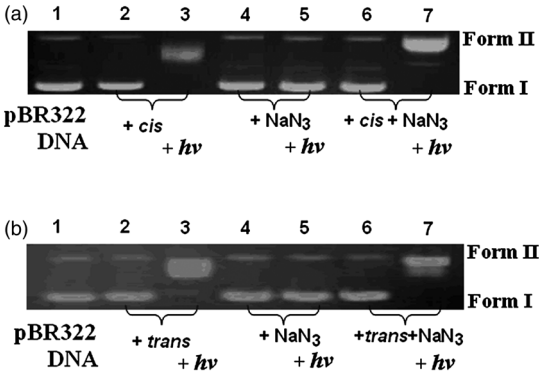

Fig. 5 Agarose gel electrophoresis comparison of the photocleavage of the (a) cis and (b) trans isomers on supercoiled pBR322 DNA with the addition of NaN_3 upon light irradiation at 420 nm. Lane 1: DNA alone. Lane 2: DNA + isomer complex. Lane 3: DNA+ isomer complex + hv. Lane 4: DNA + NaN_3. Lane 5: DNA + NaN_3+ hv. Lane 6: DNA + isomer complex + NaN_3. Lane 7: DNA+ isomer complex + NaN_3 + hv.

DNA damage for both $[Ru(OAc)(2mqn)_2NO]$ isomers (Lane 7). By contrast, NaN_3 efficiently inhibited DNA cleavage for Ru(II) polypyridyl complexes, in which $^1O_2$ was detected by an EPR spin trapping technique and $^1O_2$ caused DNA strand cleavage.[44,45]

3.4 *Photocytotoxicity*

MTT assay was conducted to evaluate the photocytotoxic potential of the isomer complexes upon photoexcitation using human cervical HeLa cancer cells as shown in Fig. 6. Upon prior incubation for 4 h in the dark and the subsequent exposure to light of 420 nm for 30 min, the trans isomer showed a moderate decrease in the cell viability with IC_{50} values of 10.0 μM under the light and 29.0 μM in the dark. The trans isomers exhibited better cytotoxicity and photocytotoxicity activity against the HeLa tumor cell line.

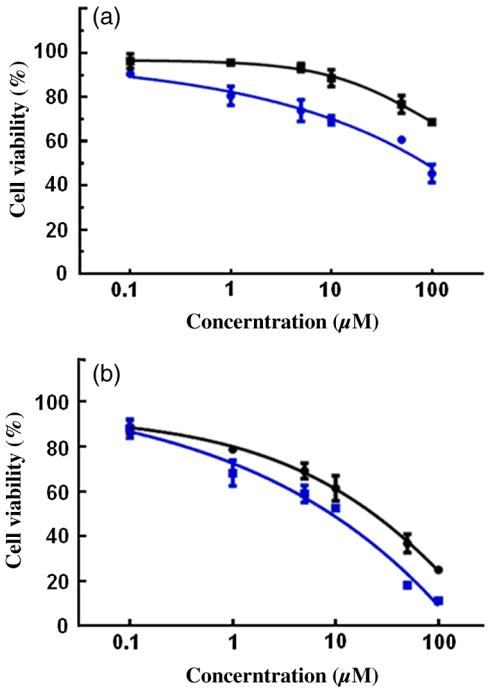

Fig. 6 Cell viability plots showing the photocytotoxicity of the (a) cis and (b) trans isomer complexes in HeLa cells on 4 h incubation in dark followed by exposure to light of 420 nm for 30 min, as determined from the MTT assay. The nonlinear fitted curves for dark-treated and photo-exposed cells are shown by black squares and blue circles for cis isomer, and black circles and blue squares for trans isomer, respectively.

Cis-platin is known to give an IC_{50} value of 7.5 μM in the dark for HeLa cells after 24 h incubation. Incubation of HeLa cells with cis-platin for 4 h in the dark and subsequent exposure to UV-A light gave IC_{50} values of 68.7 μM under UV-A light of 365 nm, thus showing no apparent PDT effect.[46] The cis isomer gave an IC_{50} value of >300 μM with the cells unexposed to light, while it gave an IC_{50} value of 100 μM with the cells exposed to light. Therefore, the cis isomers are less toxic and show very low cytotoxicity against the HeLa tumor cell line in dark, but its cytotoxicity activity increased to some extent upon photoirradiation.

4 Discussion

Several studies have implied that biological effects of NO depend on the concentration of NO in the biological milieu.[47–49] Therefore, it is very important to detect and quantitatively control NO release from an NO-donating agent at physiological targets for application in biomedicine. In order to achieve the effective regulation of physiological and pathological processes, the photodissociation of two $[Ru(OAc)(2mqn)_2NO]$ (H2mqn = 2-methyl-8-quinolinol) isomers was investigated by MALDI-TOF MS, and the spectra showed two main mass signals corresponding to the fragments of $[Ru(II)(2mqn)_2NO]^+$ with the loss of the –OAc group and $[Ru(III)(2mqn)_2]^+$ with the further loss of the NO group. The spin trapping of NO free radicals, with $Fe(MGD)_2$ as the scavenger, was also detected via EPR spectroscopy. The photoinduced NO release from $[Ru(OAc)(2mqn)_2NO]$ was confirmed and the real-time NO release upon photoirradiation at different wavelengths from visible to UV were investigated. The NO release could be controlled by using different irradiation wavelengths. Furthermore, the trans isomer produces slightly more NO upon photoirradiation than the cis isomer at the identical concentration.

In biological systems, reactive oxygen/nitrogen species have an important function for regulating cell function, signaling, and immune response; however, these species reduce cell viability in unregulated concentrations. These free radicals can cause oxidative damage to biomolecules by the loss of protein function, DNA cleavage, or lipid peroxidation, and ultimately to oxidative stress, which finally results in cell injury or death.[50] To further investigate the mechanism, the spin trapping of $^1O_2$ and $O_2^{\bullet-}$ free radicals from two $[Ru(OAc)(2mqn)_2NO]$ isomers by EPR measurements was performed upon photoirradiation. DMPO was used for $O_2^{\bullet-}$ detection and TEMPO for $^1O_2$ detection. However, in this study, no free radical signal was detected via EPR spectroscopy with and without photoirradiation, except for the NO free radicals. Therefore, in contrast to the results of the extensively studied Ru(II) polypyridyl complexes, NO free radicals and photodissociated species from $[Ru(OAc)(2mqn)_2NO]$ complexes have a great impact on the conformational change of DNA.

Both cis and trans isomers show obvious photoinduced damage on plasmid DNA; however, the trans isomer shows higher cytotoxicity activity against the HeLa tumor cell line than cis isomer. The origin of cis-/trans- effect may be attributed to

the different molecular polarity and electronic properties arising from different geometries of isomer complexes, which may lead to different behaviors of isomers in metabolism *in vivo*, transmembrane as well as different interactions with the cellular target. Furthermore, it is still needed to increase the efficiency of light absorption and the yield of nitric oxide released for isomer complexes upon photoirradiation to enhance the light-induced cellular effect. Overall, the photoactivities of different Ru complexes will give deep insight as to how to synthetically control the complex structure for the desired NO release as compared with traditional methods. These promising findings suggest that nitrosylruthenium(II) complex containing 8-quinolinol derivatived ligands as a potential NO-donor reagent will spur researchers to pursue investigations on the nitrosylruthenium(II) complexes as potential photoactivated dual-action regents with biomedicinal applications.

Acknowledgments

Research project was supported by the National Natural Science Foundation of China (J1103210). The Talent Plan of Shanxi Province and Shanxi Scholarship Council of China are gratefully acknowledged.

References

1. L. J. Ignarro et al., *Nitric Oxide: Biology and Pathobiology*, Academic Press, San Diego (2000).
2. D. Fukumura et al., "The role of nitric oxide in tumour progression," *Nat. Rev. Cancer* **6**(7), 521–534 (2006).
3. J. O. Lundberg et al., "Nitrate and nitrite in biology, nutrition and therapeutics," *Nat. Chem. Biol.* **5**(12), 865–869 (2009).
4. D. Hirst et al., "Nitric oxide in cancer therapeutics: interaction with cytotoxic chemotherapy," *Curr. Pharm. Des.* **16**(4), 411–420 (2010).
5. A. G. Tennyson et al., "Generation, translocation, and action of nitric oxide in living systems," *Chem. Biol.* **18**(10), 1211–1220 (2011).
6. C. Napoli et al., "Nitric oxide-releasing drugs," *Annu. Rev. Pharmacol. Toxicol.* **43**, 97–123 (2003).
7. P. G. Wang et al., *Nitric Oxide Donors for Pharmaceutical and Biological Applications*, Wiley-VCH, Weinheim (2005).
8. G. R. Thatcher et al., "An introduction to NO-related therapeutic agents," *Curr. Top. Med. Chem.* **5**(7), 597–601 (2005).
9. D. Hirst et al., "Targeting nitric oxide for cancer therapy," *J. Pharm. Pharmacol.* **59**(1), 3–13 (2007).
10. E. V. Stevens et al., "Nitric oxide-releasing silica nanoparticle inhibition of ovarian cancer cell growth," *Mol. Pharm.* **7**(3), 775–785 (2010).
11. K. J. Franz et al., "Nitrosyl transfer from manganese to iron in tropocoronand complexes," *Inorg. Chem.* **39**(16), 3722–3723 (2000).
12. F. Derosa et al., "Chromium(III) complexes for photochemical nitric oxide generation from coordinated nitrite: synthesis and photochemistry of macrocyclic complexes with pendant chromophores, trans-[Cr(L)(ONO)(2)]BF(4)," *Inorg. Chem.* **44**(12), 4157–4165 (2005).
13. N. L. Fry et al., "Photoactive ruthenium nitrosyls as NO donors: how to sensitize them toward visible light," *Acc. Chem. Res.* **44**(4), 289–298 (2011).
14. M. J. Rose et al., "Sensitization of ruthenium nitrosyls to visible light via direct coordination of the dye resorufin: trackable NO donors for light-triggered NO delivery to cellular targets," *J. Am. Chem. Soc.* **130**(27), 8834–8846 (2008).
15. A. C. Pereira et al., "Ruthenium-nitrite complex as pro-drug releases NO in a tissue and enzyme-dependent way," *Nitric Oxide* **24**(4), 192–198 (2011).
16. A. C. Merkle et al., "Spectroscopic analysis and photolabilization of water-soluble ruthenium(III)-nitrosyl complexes," *Dalton Trans.* **41**(26), 8047–8059 (2012).
17. Y. Y. Scaffidi-Domianello et al., "Novel cis- and trans-configured bis(oxime)platinum(II) complexes: synthesis, characterization, and cytotoxic activity," *Inorg. Chem.* **49**(12), 5669–5678 (2010).
18. C. Bartel et al., "Cellular accumulation and DNA interaction studies of cytotoxic trans-platinum anticancer compounds," *J. Biol. Inorg. Chem.* **17**(3), 465–474 (2012).
19. V. B. Arion et al., "Synthesis, x-ray diffraction structures, spectroscopic properties, and in vitro antitumor activity of isomeric (1H-1,2,4-triazole) Ru(III) complexes," *Inorg. Chem.* **42**(19), 6024–6031 (2003).
20. E. S. Antonarakis and A. Emadi, "Ruthenium-based chemotherapeutics: are they ready for prime time?," *Cancer Chemother. Pharmacol.* **66**(1), 1–9 (2010).
21. E. Alessio et al., "Ruthenium antimetastatic agents," *Curr. Top. Med. Chem.* **4**(15), 1525–1535 (2004).
22. C. G. Hartinger et al., "A new redox-active anticancer agent—preclinical development and results of a clinical phase I study in tumor patients," *Chem. Biodivers.* **5**(10), 2140–2155 (2008).
23. A. Levina et al., "Recent developments in ruthenium anticancer drugs," *Metallomics* **1**(6), 458–470 (2009).
24. K. Miki et al., "Crystal structures of three geometrical isomers of [Ru(OAc)(2mqn)2 NO] (OAc = acetate, H2mqn = 2-methyl-8-quinolinol) and their thermal isomerization reactions," *Inorg. Chim. Acta* **257**(1), 3–10 (1997).
25. H. Wang et al., "Electronic effects of the substituent group in 8-quinolinolato ligand on geometrical isomerism for nitrosylruthenium(II) complexes," *Inorg. Chim. Acta* **299**(1), 80–90 (2000).
26. M. J. Frisch et al., *Gaussian 09, Revision C.01*, Gaussian, Inc., Wallingford, CT (2009).
27. R. Dennington et al., *GaussView, Version 5*, Semichem Inc., Shawnee Mission, KS (2009).
28. C. Lee et al., "Development of the Colle-Salvetti correlation-energy formula into a functional of the electron density," *Phys. Rev. B* **37**(2), 785–789 (1988).
29. A. D. Becke, "Density-functional thermochemistry. III. The role of exact exchange," *J. Chem. Phys.* **98**(7), 5648–5652 (1993).
30. A. F. Vanin et al., "Why iron-dithiocarbamates ensure detection of nitric oxide in cells and tissues," *Nitric Oxide* **15**(4), 295–311 (2006).
31. S. Porasuphatana et al., "Differential effect of buffer on the spin trapping of nitric oxide by iron chelates," *Anal. Biochem.* **298**(1), 50–56 (2001).
32. B. Gopalakrishnan et al., "Detection of nitric oxide and superoxide radical anion by electron paramagnetic resonance spectroscopy from cells using spin traps," *J. Vis. Exp.* **66**, 2810 (2012).
33. S. Pou et al., "Spin trapping of nitric oxide by ferro-chelates: kinetic and in vivo pharmacokinetic studies," *Biochim. Biophys. Acta* **1427**(2), 216–226 (1999).
34. M. K. Nazeeruddin et al., "Combined experimental and DFT-TDDFT computational study of photoelectrochemical cell ruthenium sensitizers," *J. Am. Chem. Soc.* **127**(48), 16835–16847 (2005).
35. Q. J. Pan et al., "Structures, spectroscopic properties and redox potentials of quaterpyridyl Ru(II) photosensitizer and its derivatives for solar energy cell: a density functional study," *Phys. Chem. Chem. Phys.* **13**(32), 14481–14489 (2011).
36. D. A. Lutterman et al., "Theoretical insight on the S→O photoisomerization of DMSO complexes of Ru(II)," *J. Phys. Chem. A* **113**(41), 11002–11006 (2009).
37. L. Li et al., "Ruthenium complexes containing bis-benzimidazole derivatives as a new class of apoptosis inducers," *Dalton Trans.* **41**(4), 1138–1141 (2012).
38. C. Tan et al., "Synthesis, structures, cellular uptake and apoptosis-inducing properties of highly cytotoxic ruthenium-Norharman complexes," *Dalton Trans.* **40**(34), 8611–8621 (2011).
39. T. F. Chen et al., "Ruthenium polypyridyl complexes that induce mitochondria-mediated apoptosis in cancer cells," *Inorg. Chem.* **49**(14), 6366–6368 (2010).
40. C. Tan et al., "Nuclear permeable ruthenium(II) β-carboline complexes induce autophagy to antagonize mitochondrial-mediated apoptosis," *J. Med. Chem.* **53**(21), 7613–7624 (2010).
41. A. Srishailam et al., "Synthesis, DNA-binding, cytotoxicity, photo cleavage, antimicrobial and docking studies of Ru(II) polypyridyl complexes," *J. Fluoresc.* **23**(5), 897–908 (2013).
42. X. L. Zhao et al., "Synthesis, pH-induced 'on-off-on' luminescence switching, and partially intercalative DNA-binding and DNA photocleavage properties of an β-D-allopyranoside-grafted ruthenium(II) complex," *J. Inorg. Biochem.* **113**, 66–76 (2012).

43. J. F. Kou et al., "Chiral ruthenium(II) anthraquinone complexes as dual inhibitors of topoisomerases I and II," *J. Biol. Inorg. Chem.* **17**(1), 81–96 (2012).
44. Q. X. Zhou et al., "Ruthenium(II) terpyridyl complexes exhibiting DNA photocleavage: the role of the substituent on monodentate ligand," *J. Phys. Chem. B* **113**(33), 11521–11526 (2009).
45. X. L. Zhao et al., "DNA- and RNA-binding and enhanced DNA-photocleavage properties of a ferrocenyl-containing ruthenium(II) complex," *J. Inorg. Biochem.* **107**(1), 104–110 (2012).
46. A. Hussain et al., "Photocytotoxic lanthanum(III) and gadolinium(III) complexes of phenanthroline bases showing light-induced DNA cleavage activity," *Inorg. Chem.* **49**(9), 4036–4045 (2010).
47. D. A. Wink, "Chemical biology of nitric oxide: insights into regulatory, cytotoxic, and cytoprotective mechanisms of nitric oxide," *Free Radic. Biol. Med.* **25**(4), 434–456 (1998).
48. D. Mancardi, "The chemical dynamics of NO and reactive nitrogen oxides: a practical guide," *Curr. Mol. Med.* **4**(7), 723–740 (2004).
49. B. Bonavida, "Dual role of NO donors in the reversal of tumor cell resistance and EMT: downregulation of the NF-κB/Snail/YY1/RKIP circuitry," *Nitric Oxide* **24**(1), 1–7 (2011).
50. C. C. Winterbourn, "Reconciling the chemistry and biology of reactive oxygen species," *Nat. Chem. Biol.* **4**(5), 278–286 (2008).

Jiao Liu received her BS degree from Shanxi University, China, and is currently a graduate student at the Key Laboratory of Chemical Biology and Molecular Engineering of the Education Ministry, Institute of Molecular Science, Shanxi University. Her current research involves cell biology and biomedical optics.

Qingqing Duan received her BS degree from Taiyuan University of Science and Technology, China, and is currently a graduate student at the State Key Lab of Quantum Optics and Quantum Optics Devices, Institute of Opto-Electronics, Shanxi University. Her current research involves laser biology and biomedical optics.

Jianru Wang received her MS degree from Beijing University of Technology, China, in 2007, and she was an assistant professor at Shanxi Medical University. She is currently a graduate student at State Key Lab of Quantum Optics and Quantum Optics Devices, Institute of Opto-Electronics, Shanxi University. Her current research involves laser biology and biomedical optics.

Zhen Song received her PhD degree in 2014 from Key Laboratory of Chemical Biology and Molecular Engineering of the Education Ministry, Institute of Molecular Science, Shanxi University. She is currently an assistant professor at Taiyuan Normal University, China. Her current research involves bioinorganic chemistry and chemical biology.

Xiaoyan Qiao received her PhD degree from Tianjin University, China, in 2007. She is currently an associate professor in the College of Physics and Electronics Engineering, Shanxi University. Her current research involves biophysics and biomedical optics.

Hongfei Wang received his PhD degrees from Nanjing University, China, in 1996 and from Rikkyo University, Japan, in 2001. He was a postdoctoral research associate in the Institute of Physical and Chemical Research (RIKEN), Japan. He is presently a professor at Shanxi University, China. His current research involves photophysics and photochemistry, as well as biomedical optics.